JOURNAL OF PHYSIOLOGY AND PHARMACOLOGY 2017, 68, 4, 573-583
www.jpp.krakow.pl

R. PINGWARA[1,2], K. WITT-JURKOWSKA[1], K. ULEWICZ[1], J. MUCHA[1], K. TONECKA[2], Z. PILCH[2], B. TACIAK[1], K. ZABIELSKA-KOCZYWAS[3], M. MORI[4], S. BERARDOZZI[4,5], B. BOTTA[5], T.P. RYGIEL[2], M. KROL[1]

INTERFERON LAMBDA 2 PROMOTES MAMMARY TUMOR METASTASIS *VIA* ANGIOGENESIS EXTENSION AND STIMULATION OF CANCER CELL MIGRATION

[1]Department of Physiological Sciences, Faculty of Veterinary Medicine, Warsaw University of Life Sciences, Warsaw, Poland; [2]Department of Immunology, Centre for Biostructure Research, Medical University of Warsaw, Warsaw, Poland; [3]Department of Small Animal Diseases with Clinic, Faculty of Veterinary Medicine, Warsaw University of Life Sciences, Warsaw, Poland; [4]Center for Life Nano Science@Sapienza, Italian Institute of Technology, Rome, Italy; [5]Department of Chemistry and Technology of Drugs, Sapienza University of Rome, Rome, Italy

Myeloid-derived suppressor cells (MDSCs) support tumor development by stimulation of angiogenesis and immune response inhibition. In our previous study, we showed that interferon lambda 2 (IFN-λ2), secreted by MDSCs, enhances production of pro-angiogenic factors by cancer cells *via* phosphorylation of STAT3 and therefore promotes blood vessels formation. In the present study IFN-λ2 level was evaluated by ELISA in serum of tumor-bearing mice, whereas its expression in MDSCs isolated from the lungs with metastatic tumors and normal lungs was assessed by qPCR. The effect of IFN-λ2 on mouse mammary cancer cells motility was tested in Boyden chamber migration assay. In order to evaluate its pro-angiogenic function we performed *in vitro* tubule formation assay and *in ovo* angiogenesis assay on chicken embryo chorioallantoic membrane (CAM). Moreover, in order to design small molecule inhibitors of IFN-λ2 and its receptor we performed molecular modeling followed by the identification of potential natural inhibitors. Then, we examined their ability to inhibit angiogenesis *in vitro*. Our results showed that IFN-λ2 predisposed mouse mammary cancer cells to migration *in vitro*. It also enhanced angiogenesis induced by mouse mammary cancer cells *in vitro* and *in ovo*. For the first time we selected potential IFN-λ2 inhibitors and we validated that they were capable to abolish pro-angiogenic effect of IFN-λ2, similarly to blocking antibodies. Therefore, IFN-λ2 and its receptor may become targets of anti-cancer therapy, but their mechanism of action requires further investigation.

Key words: *interferon lambda, interleukin-28, breast cancer, angiogenesis, metastasis, cell migration, endothelial cells, myeloid-derived suppressor cells*

INTRODUCTION

Myeloid-derived suppressor cells (MDSCs) constitute a heterogeneous population of immature myeloid cells. In physiological conditions MDSCs can differentiate predominantly into granulocytes, or macrophages. Their main phenotypic hallmark is the capacity to suppress proliferation of T lymphocytes. In healthy individuals they are present in spleen and bone marrow, but their number in blood is very low. In tumor-bearing individuals, MDSCs are mobilized from bone marrow and migrate to the tumor. They are actively recruited to the tumor microenvironment by various chemokines in a similar manner as other cells (1-3). In the tumor tissue MDSCs are involved in tumor development and metastasis due to immunosuppressive and pro-angiogenic activity. MDSCs activate signal transducer and activator of transcription (STAT3) in cancer cells leading to secretion of pro-angiogenic factors such as: vascular endothelial growth factor (VEGF), matrix metalloproreinases (MMPs) and interleukins (IL-1β, IL-6, IL-10, IL-23) (4). Results of our previous studies suggested that MDSCs are able to induce above mentioned changes in cancer cells via IFN-λ2 (5).

The IFN-λ2 (IL-28A) is a 20kDa molecular mass cytokine, which has been described for the first time in 2003. Similarly to IFN-λ1 (IL-29), IFN-λ3 (IL-28B) and IFN-λ4, it belongs to the III type interferon's group, and it is classified as a member of IL-10 interleukin family (6-8). It has been shown that IFN-λ2 plays a crucial role in response to viral infections (9, 10). Polymorphism of *IFN-λ3* gene is one of the factors determining the course of disease and sensitivity to interferon therapy (11, 12). Published data suggest that IFN-λ2 may be involved in tumor development. IFN-λ2, similarly to IFN-α have high anti-tumoral activity. Its beneficial effect has been observed both *in vitro* and *in vivo* in many various tumor models, for example: melanoma, lung cancer, neuroendocrine tumors, sarcoma, colorectal and hepatocellular carcinoma (13, 15). It has been shown that IFN-λ2 had antitumor activity by inhibition of cancer cells proliferation and induction of apoptosis (16-20). On the other hand, listed above sarcomas with high expression of IFN-λ2 showed slower growth and ability to metastasize (18).

Moreover, IFN-λ2 enhances local immune response against tumor cells (21). However, the role of IFN-λ2 seems to be unclear in tumor development because it is known to activate JAK/STAT signaling pathway (6, 7). Our previous study showed that IFN-λ2 increases phosphorylation of STAT3 in cancer cells and subsequent secretion of pro-angiogenic factors such as: VEGF, MMPs and IL-18 (5). Treatment of canine mammary cancer cells and human bladder cancer cells with IFN-λ2 increases cell migration *in vitro* (5, 22). Tumors from patients with advanced stage of bladder cancer have higher expression of IFN-λ2 (23). Importantly, pro-tumoral activity of IFN-λ1 was also published. It has been shown to promote proliferation of leukemic B cells (24).

In this study we investigated the role of IFN-λ2 in tumor development focusing on tumor metastasis and angiogenesis using mouse mammary cancer model *in vitro*. After molecular 3D modeling, we identified *in silico* a number of natural small molecular inhibitors of IFN-λ2/IFN-λ2R interaction that were subsequently tested *in vitro*. We also verified if levels of IFN-λ2 in serum and its expression in MDSCs could constitute potential diagnostic approach.

MATERIALS AND METHODS

Cell lines and cell culture

Mouse tumor cell lines were purchased from ATCC and were cultured under optimal conditions: in RPMI-1640 (EMT6, 4T1) or DMEM medium (EL-4, B78, B16F10) supplemented with 10% (v/v) heat-inactivated fetal bovine serum (FBS), penicillin-streptomycin (50 U/mL), and fungizone (2.5 mg/ml). The human umbilical venous endothelial cell line (HUVEC) was purchased from Life Technologies (USA). HUVEC cells were cultured in 200PRF medium (Gibco, USA) with Low Serum Growth Supplement (LSGS) (Gibco) in standard culture conditions in an atmosphere of 5% CO_2 and 95% humidified air at 37°C. For the 3D tubule formation assays only early passages of HUVEC cells were used (P3–P6). If not stated otherwise, all cell culture reagents were purchased from Sigma Aldrich (USA).

Animal experiments

C57BL/6 mice were purchased from the SPF-unit of the Mossakowski Medical Research Centre Polish Academy of Sciences (Warsaw, Poland). For the experiments, mice (all females 8 – 12 weeks old) were housed in the conventional, non-SPF facility of the Medical University of Warsaw. All *in vivo* experiments were performed in accordance with the legal guidelines and approved by the Local Ethics Committee. In the intravenous model mice were injected into the tail vein with 1.5×10^5 of B16F10 melanoma cells or EL4 lymphoma. B78 melanoma cells were inoculated subcutaneously 1.5×10^5 in 50 µl of Matrigel Growth Factor Reduced (Corning®, LifeSciences). After 14 days, mice were sacrificed, blood and lungs containing tumor cells were used for further analysis.

Fluorescence-activated cell sorting (FACS)

Lungs were cut into small pieces and digested for 30 min at 37°C using Collagenase type IV (600U) (Sigma) and (400U) DNAse (Sigma). Next, tissues were dissociated using a gentleMACS Dissociator (Miltenyi), and filtered through a 70 µm cell strainer, washed with PBS containing 2 mM EDTA and 1% FBS, centrifuged and stained. When necessary, erythrocytes were lysed using buffer containing 155 mM NH_4Cl, 10 mM NaH_2CO_3, 0.1 mM EDTA, pH 7.3. For staining, cells were blocked in 5% normal rat serum and stained with fluorescently labeled monoclonal antibodies against: anti-CD11b (clone M1/70, 53-0112-82), (eBioscicence), anti-CD45.2 (clone 104, 562129), anti-Gr-1 (clone RB6-8C5, 552093) (BD Pharmingen). Cells were analyzed on FACS Aria III cytometer-sorter (Beckton Dickinson) using FACSDiva software 6.0. The $Gr1^+CD11b^+CD45^+$ cells were gated, counted and sorted for RNA isolation.

Real-time qPCR and ELISA

Total-RNA was isolated from the FACS-sorted MDSCs from the lung metastases of B16F10 using Total RNA Kit (A&A Biotechnology, Poland) according to the manufacturer's protocol. RNA quantity was measured using the NanoDrop (NanoDrop Technologies, USA). Moreover, its purity and integrity was evaluated by Bioanalyzer (Agilent, USA). Used primers sequence were: IFN-λ2 (F:TAGAAGGTGGCGAAAAGTGA, R:CTGGCTCCACTTCAAAAAGGTA,),
GAPDH (F:GCTTAAGAGACAGCCGCATCT,
R:CGACCTTCACCATTTTGTCTACA). Quantitative RT-PCR was performed using a fluorogenic Lightcycler Fast Strand DNA SYBR Green kit (Roche). Data were analyzed using the comparative Ct method. Relative transcript abundance of the gene equals ΔCt values ($\Delta Ct = Ct_{reference} - Ct_{target}$). Relative changes in transcript are expressed as ΔΔCt values ($\Delta\Delta Ct = \Delta Ct_{control} - \Delta Ct_{examined}$). The experiment was repeated three times. In order to detect IFN-λ2 in serum, Mouse IL-28 ELISA Ready-SET-Go!® (eBioscicence) was used, according to manufacturer's instructions. The experiment was repeated three times.

Molecular modeling

Crystallographic structures of the IFN-λ2R/IFN-λ1 adduct coded by PDB ID 3OG4 and 3OG6 were used as template in the generation of a 3D structure of IFN-λ2/IFN-λ2R complex by homology modeling (25). To this aim, the MODELER(19) program (version 9.10) was used (26). Further, MD simulations were performed with AMBER12 software (27), using settings described elsewhere (28-30). To identify possible hot-spots for ligand interaction, IFN-λ2R residues closer than 4 Å from the surface of IFN-λ2 were mutated to alanine according to the computational alanine scanning protocol implemented in AMBER12. Theoretical affinity between IFN-λ2 and mutated IFN-λ2R was then estimated by means of the MM-PBSA method and compared to the affinity of the wild-type IFN-λ2/IFN-λ2R complex (31). The library of natural products and their derivatives (available at the laboratories of Professor Bruno Botta, Sapienza University of Rome, Italy) was screened *in silico* by molecular docking towards the identified druggable pocket. The FRED docking program from OpenEye (version 3.2.1) was used in molecular docking simulations (32, 33). Ligand conformational analysis was performed with OMEGA2 from OpenEye using default settings (34, 35).

Source of compounds and plant material

The stem bark of *Vochysia divergens* Pol. (Vochysiaceae) was collected in Corumba, Mato Grosso do Sul, Brasil. The roots of *Ficus thonningii* Blume (Moraceae) were collected in Bagante, Cameroon.

24-hydroxytormentic acid, 6-prenylaromadendrin and curcumin belong to the *in house* library. Chemical identity of bioactive compounds was assessed by IR, UV, ESI-MS, ^{1}H-NMR, and ^{13}C-NMR experiments, which proved to be in agreement with the literature data available for the compounds (36, 37). The purity of the compound, checked by HPLC, was

higher than 95%. 24-hydroxytormentic acid (methyl ((1R,2S,4αS,6αS,6βR,9S,10R,11R,12αR,14βS)-1,10,11-trihydroxy-9-(hydroxymethyl)-1,2,6α,6b,9,12α-hexamethyl-1,3,4,5,6,6α,6β,7,8,8α,9,10,11,12,12α,12β,13,14βoctadecahydropicene-4α(2H)-carboxylic acid) was obtained from *Vochysia divergens* by following the procedure already described (38). The powdered stem bark (4.0 kg) was exhaustively extracted with cold EtOH. After evaporation, a mixture of MeOH/H_2O 95:5 (250 mL) was added to a part (20 g) of the EtOH extract, and filtered. Evaporation of the soluble portion (14 g) and washing with cold $CHCl_3$ yielded a soluble fraction (8 g) and an insoluble fraction (6 g). Repeated column chromatography of the insoluble fraction on SiO_2 yielded 24-hydroxytormentic acid (700 mg) by elution with a gradient of MeOH in EtOAc, hexane/EtOAc 7:3, $CHCl_3$/MeOH/H_2O 19.5:8.5:2.3, and EtOAc/MeOH, 9:1.6-prenylaromadendrin ((2R,3R)-3,5,7-trihydroxy-2-(4-hydroxyphenyl)-6-(3-methylbut-2-en-1-yl)chroman-4-one) was obtained from *Ficus thonningii* by following the procedure already described (39). The dried and powdered roots (400 g) of *F. thonningii* were extracted with MeOH/CH_2Cl_2 1:1 (v/v) at room temperature for 48 h and MeOH for 8 h. The combined extracts (25 g) were subjected to column chromatography over silica gel 60 (100 g) and eluted with hexane/EtOAc and $CHCl_3$/MeOH of increasing polarity. Fifty fractions of 200 mL each were collected, concentrated, monitored by TLC and similar ones pooled to give a total of six fractions (A–F). Fraction C (1 g, hexane/EtOAc 75:25 to 70:30), was passed through Sephadex LH-20 eluted with $CHCl_3$–MeOH 70:30 to give 6-prenylaromadendrin (50 mg).

Curcumin ((1E,6E)-1,7-bis(4-hydroxy-3-methoxyphenyl) hepta-1,6-diene-3,5-dione) was purchased from Sigma Aldrich.

Chemicals and instruments

The solvents, having an analytical grade or HPLC grade, were purchased from Sigma Aldrich. All reagents were used without further purification. Chromatography was carried out on silica gel (70 – 230 mesh). All chromatography fractions were monitored by thin-layer chromatography (TLC), and silica gel plates with fluorescence F254 were used.

Melting point was taken in open capillaries on a Buchi Melting Point B-545 apparatus and was uncorrected. Infrared spectrum was recorded on a FT-IR spectrometer. UV spectrum was recorded on a JASCO V-550 spectrophotometer. ^{1}H NMR and ^{13}CNMR spectra were recorded using a Bruker 400 Ultra ShieldTM spectrometer (operating at 400 MHz for ^{1}H and 100 MHz for ^{13}C) using $CDCl_3$ as solvent and tetramethylsilane (TMS) as internal standard. Chemical shifts are reported in parts per million. Multiplicities are reported as follows: singlet (s), doublet (d), multiplet (m), and broad doblet (brd). Mass spectrometry was performed using a Thermo Finnigan LXQ linear ion trap mass spectrometer, equipped with an electrospray ionization (ESI) ion source bearing a steel needle.

MTT assay

Metabolic activity assay was performed in 96-well plate. The EMT6 cells were plated at the density of 2.5×10^4 cells per well whereas 4T1 cells were plated at the concentration of 5×10^4 cells per well. The cells were cultured for 24 hours in the full RPMI1640 medium with all previously selected inhibitors in virtual screening of the natural compounds library. After the first round of screening, particular attention has been paid on: 6-prenylaromadendrin (2, 6, 8 µM) 24-hydroxytormentic acid (2, 6, 8 µM) and curcumin (0,1, 10, 20 µM).These compounds have been tested more extensively. Subsequently, the cells are incubated in 0.5 mg/ml tetrazolium salt MTT Diluted in phenol red-free RPMI 1640 medium (Sigma-Aldrich) for 4 hat 37°C. Formazan was dissolved by DMSO and subsequently its concentration was measured by the photometric absorbance at 570 nm and reference absorbance at 650 nm using plate reader Infinite 200 PRO TecanTM (TECAN, Mannedorf, Switzerland). The experiment was repeated three times.

Migration assay

Equal numbers of cells (2.5×10^5 cells) treated with IFN-λ2 (400 ng/mL) (R&D Systems, USA) or with blocking antibodies for IFN-λ2R (Abcam, USA) in RPMI 1640 medium containing 0.2% FBS were added to the BD Falcon FluoroBlock 24-Multiwell Insert Plates (8 micron pore size) (BD Biosciences). Solution of 10% FBS in medium was used as chemoattractant in the basal chambers. Culture medium without cells was used as a negative control. Assay plates were incubated for 22 hours at standard culture conditions. Incubation medium was carefully removed from the apical chamber and insert system was transferred into a second 24-well plate containing 500 µl of 2.5 µg/ml Calcein AM in Hanks' Balanced Salt solution (HBSS). Plates were incubated for 1 hour at standard culture conditions. The fluorescence of invaded cells was measured at excitation wavelength 485 nm and emission wavelength 530 nm using a fluorescent plate reader with bottom reading capabilities, Infinite 200 PRO Tecan (TECAN, Switzerland). To visualize the invaded cells, a fluorescence microscope (Olympus BX60) at 4× magnification was used. The experiment was repeated three times.

Tubule formation assay (angiogenesis in vitro assay)

Culture plates (24 wells; Corning Inc.) were coated for 30 min at 37°C with Matrigel Growth Factor Reduced (Corning®, LifeSciences). Subsequently, HUVECs were plated at the density of 9×10^4 cells/well. As a positive control the LSGS-supplemented Medium 200PRF was used, whereas a negative control constituted LSGS-supplemented medium with 30 mM Suramin (Sigma-Aldrich). Mouse mammary tumor cells were cultured for 48 hours in full RPMI 1640 Medium with IFN-λ2 (400 ng/mL) with or without one of the following inhibitors: 6-prenylaromadendrin (8 µM), 24-hydroxytormentic acid (6 µM), curcumin (0.1 µM) or anti-IFN-λ2R blocking antibody (Abcam, USA). The IFN-λ2 alongside with inhibitors were administered twice during the assay. Tubule formation (by HUVEC) was observed after 6 h culture on Matrigel in the presence of non-supplemented Medium 200 PRF and cancer cell-conditioned medium (at 1:1 ratio). The experiment was performed six times. The length of formed tubules was measured using ImageJ software (National Institutes of Health, USA).

In ovo angiogenesis assay

The chick embryos (Ross 308 line, Pankowski Jan Poultry Hatchery, Poland) were held in the CO_2 incubator (SMA Coudelou FOR 37210, France) under standard conditions (65% humidity, 5% CO_2 and 37.5°C) as soon as the embryogenesis starts. On the 5th day of incubation and 5 mm × 5 mm 'window' was made in the eggshell on the blunt end on each of the egg. The parchment-like membrane was carefully taken out and a sterile silicon ring was put into the CAM of each egg in aseptic conditions. Sterilized, medium-hard silicon rings (7 mm in external, 5 mm in internal diameter, 2 mm thick), were specially designed for this experiment and produced by Zegir PTHU (Poland). The 'window' in the egg's shell was closed using Polopor (Viscoplast, Poland) - a special adhesive tape with high air and water vapor. After 24 and 48 hours eggs were candled to check the vitality and estimate the mortality associated with manual manipulation. The silicon rings

were put into CAM two days before the start of the experiment to exclude the mortality of chick embryos caused by blood vessel damage and possible overexpressed inflammatory reaction due to ring placing. On the 7th day of incubation, medium conditioned by cancer cells (with or without IFN-λ2) was injected into the silicon rings, at least 20 chick embryos per treatment. Seven chick embryos were used as a negative control (inoculated with only 25 ml of culture medium per egg). An average chick embryo's vitality was about 85%. Medium as exactly injected into the silicon rings. Eggs are candled 24 and 48 hours later to check their survival. On the 12th day of incubation chick embryos are examined with the video otoscope (Welch Allyn MacroView™ Veterinary Otoscope 71032, USA) for blood vessels growth.

Statistical analysis

The statistical analysis was conducted using Prism version 5.00 software (GraphPad Software, California, USA). The one-way ANOVA and Tukey HSD (Honestly Significant Difference) post-hoc test, Dunnett's test and t-test were applied as well as regression analysis. The P-value < 0.05(*) was regarded as significant whereas P-value < 0.01(**) and P-value < 0.001(***) as highly significant.

RESULTS

Interferon-λ2 expression in myeloid-derived suppressor cells isolated from the lungs with metastatic tumors and interferon-λ2 level in the blood of tumor-bearing mice

Flow cytometric analysis of cells isolated from the lungs with B16F10 metastatic tumors showed that MDSCs (Gr-1$^+$CD11b$^+$CD45.2$^+$) constituted 13.4% (± 1.9) of all leukocytes, however in control mice only 5.9% (*Fig. 1A*). The expression of *Ifn-λ2* in MDSCs sorted from the lungs was as follows: 0.0108 ± 0.0029 in B16F10 tumor-bearing mice whereas 0.0013 ± 0.0007 in control mice (*Fig. 1B*). The level of IFN-λ2 protein in serum

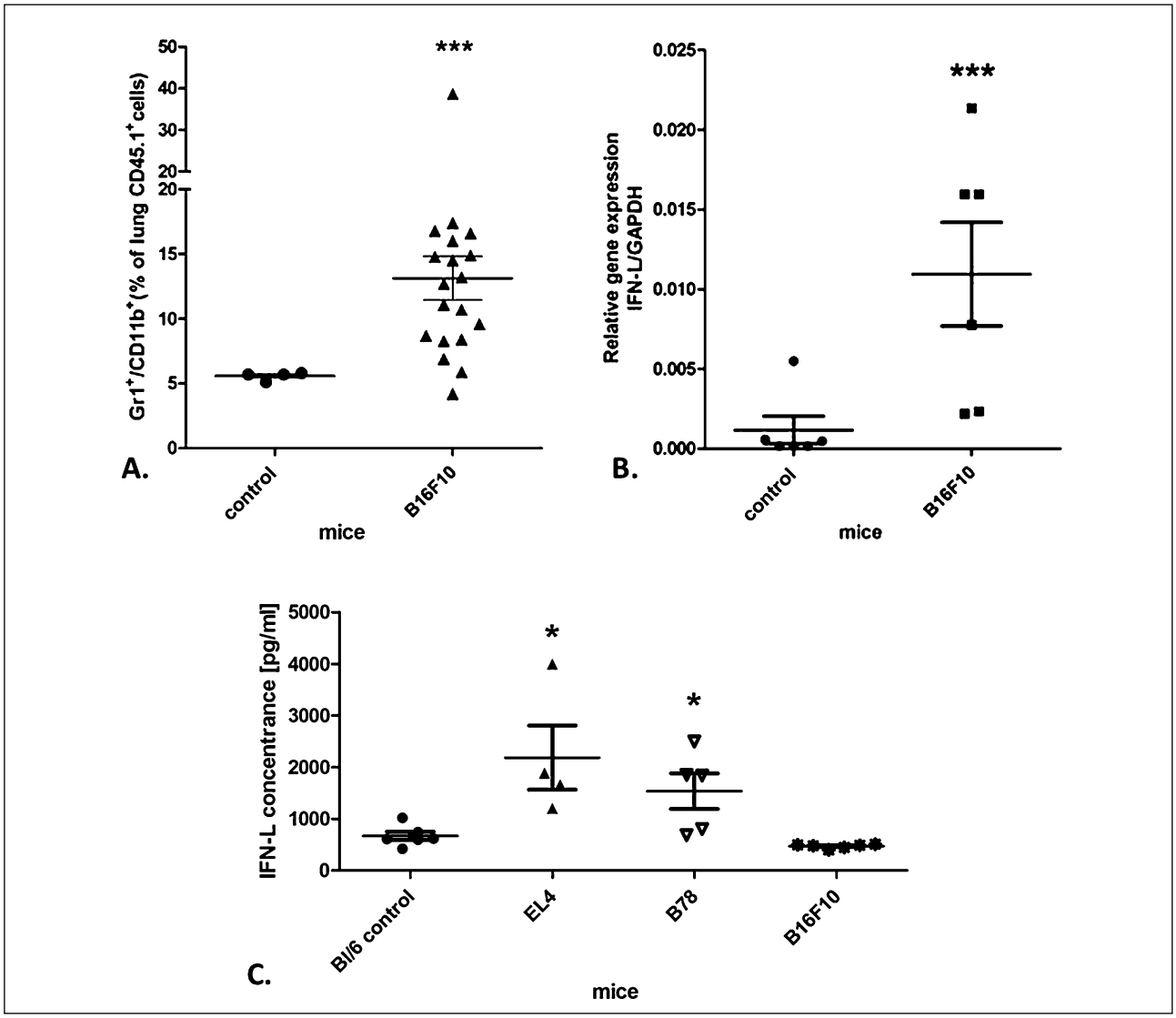

Fig. 1. (*A*). Percentage of MDSCs (CD45.2$^+$Gr-1$^+$CD11b$^+$) in the lungs of control mice and mice with B16F10 tumor. (*B*) Expression of *Ifn-λ2* in MDSCs isolated from the lungs of control mice and B16F10 tumor-bearing mice with lung metastases 14 days after inoculation with tumor cells (lung metastases were confirmed by necropsy). (*C*) Concentration of IFN-λ2 in the serum of control mice and mice with EL4, B78 and B16F10 tumors. * means P < 0.05; *** means P < 0.001.

(*Fig. 1C*) was as follows: 2154.8 pg/mL ± 598,3 in EL4 model; 1546.7 pg/mL ± 366.1 in B78 model; 474.5 pg/mL in B16F10 model; and 648.5 pg/mL ± 76 in control mice.

Interferon-λ2 increases cancer cell migration

Migration assay in Boyden Chambers showed that IFN-λ2 increased migration of EMT6 and 4T1 cells (*Fig. 2*). The mean fluorescence related to cell migration was 713.00 ± 14.14 in EMT6 cell line (compared with 473.5 ± 144.69 in control) and 139.50 ± 6.36 in 4T1 cell line (compared with 119.65 ± 12.72 in control). The IFN-λ2R blocking antibodies abolished this effect (463.67 ± 63.89 in EMT6 cell line and 111.41 ± 4.86 in 4T1 cell line).

Interferon-λ2 promotes angiogenesis

Results of the tubule formation assay indicated that EMT6 and 4T1 mice mammary cancer cells induced *per se* slight tubule formation by endothelial cells (HUVECs). Their treatment with IFN-λ2 increased 3D angiogenesis by endothelial cells (*Fig. 3A*). On the other hand, treatment of these cancer cells with IFN-λ2 and IFN-λ2R blocking antibodies completely abolished this effect (*Fig. 3A*).

The MTT assay (*Fig. 3B*) showed that percentage of live HUVEC cells treated with medium conditioned with cancer cells pre-treated with IFN-λ2 was higher than in case of medium conditioned with cancer cells untreated with IFN-λ2. The HUVEC cells viability was as follows: EMT6 pre-treated with IFN-λ2 conditioned medium - 221.39%, EMT6 conditioned medium: 102.65% and 4T1 pre-treated with IFN-λ2 conditioned medium - 125.78%, 4T1 conditioned medium - 96.81%. The *in ovo* angiogenesis assay showed that medium conditioned with EMT6 or 4T1 cells pre-treated with IFN-λ2 induced formation of new blood vessels on CAM. Conditioned medium collected from culture of the control cells that were not pre-treated with IFN-λ2 also induced angiogenesis, however this effect was less clear (*Fig. 4A* and *4B* left panel).

Identification of small molecule inhibitors of interferon-λ2/interferon-λ2R interaction

In order to select small molecules potentially able to inhibit the formation of IFN-λ2/IFN-λ2R complex, we performed a set of molecular simulations. First, we generated a 3D structure of the IFN-λ2/IFN-λ2R complex by homology modeling, using as template the available crystallographic structures of the IFN-λ2R/IFN-λ1 complex (PDB IDs: 3OG4, 3OG6) (25). Even though IFN-λ2R has been co-crystallized in complex with IFN-λ1, sequence and structural analysis revealed that IFN-λ1 and IFN-λ2 ligands share a very common sequence and overall architecture, particularly showing high conservation of residues directly involved in contacting IFN-λ2R. Thus, the high sequence identity between IFN-λ1 and IFN-λ2 permits the generation of a reliable IFN-λ2/IFN-λ2R homology model (*Fig. 5A* and *5B*), which can be used in drug design exercises. Then, molecular dynamics (MD) simulations (100 ns) were performed with AMBER12 software to relax the initial model in physiological conditions, as well as to highlight key determinants and hot-spots for IFN-λ2 and small molecules binding to the receptor IFN-λ2R through a computational alanine scanning study. Overall, molecular simulations show a druggable hydrophobic pocket on the IFN-λ2R surface, which is notably located at the binding interface to IFN-λ2 ligand. This pocket may be targeted by small molecule inhibitors of IFN-λ2/IFN-λ2R interaction (*Fig. 5A* and *5B*). Moreover, this pocket contains residues whose mutations to alanine proved to impair the overall affinity of IFN-λ2 for its receptor *in silico* (namely Lys75, Tyr73, Phe101, and Glu102, residue numbering as in PDB ID: 3OG6 - see *Fig. 5A* and *5B*), thus representing a suitable target pocket in our drug design study.

Potential inhibitors of IFN-λ2/IFN-λ2R interaction were searched among an *in house* library of natural compounds and their derivatives, which is endowed with a noticeable chemical diversity and has been already used with success in prior drug discovery studies (40-43). Virtual screening of the *in house*

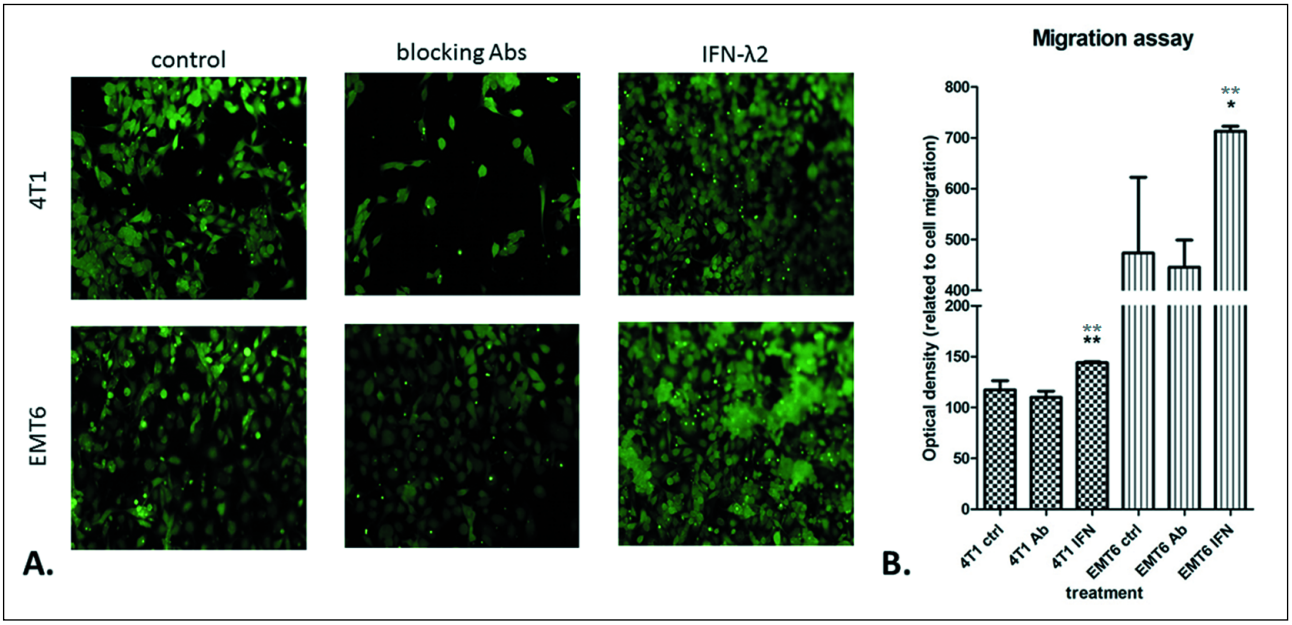

Fig. 2. (*A*) Migration assessed by fluorescence microscopy *in vitro* in Boyden chambers of control 4T1 and EMT6 cancer cells, cells treated with IFN-λ2 or IFN-λ2 with blocking antibodies and (*B*) graph showing mean fluorescence of migrating 4T1 and EMT6 cells (control and treated with IFN-λ2 either IFN-λ2 and blocking antibodies). * means $P < 0.05$; *** means $P < 0.001$. Black * relative to 4T1/EMT6 group and grey * relative to anti-IFN-λ2R antibody group.

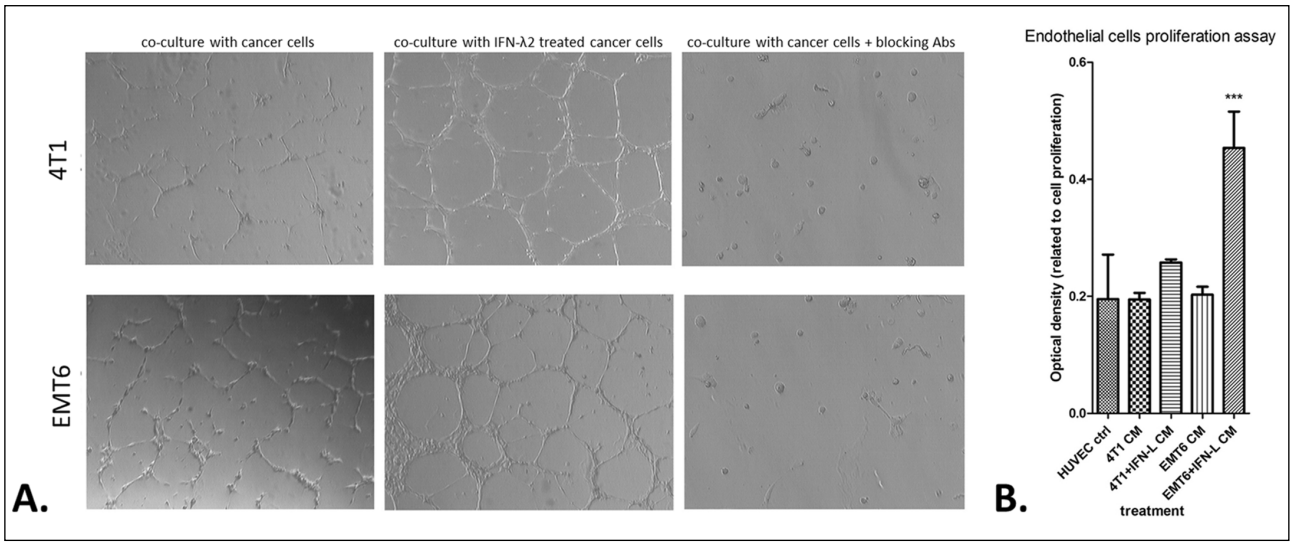

Fig. 3. (*A*) Angiogenesis assay *in vitro* (3D tubule formation assay) showing differences in 3D vessel formation by endothelial cells grown in indirect co-culture with 4T1 either EMT6 mice mammary cancer control cell lines (in Boyden chambers) and the same cells treated with IFN-λ2 either IFN-λ2 and IFN-λ2 blocking antibody. (*B*) Endothelial cells proliferation assay: HUVEC ctrl - endothelial cells cultured in standard conditions; 4T1 CM or EMT6 CM - endothelial cells treated with 20% 4T1 or EMT6 - conditioned medium (CM); and 4T1 + IFN-λ2 CM or EMT6 + IFN-λ2 CM - endothelial cells treated with 20% conditioned medium of 4T1 either EMT6 cell treated with IFN-λ2. * and *** indicates $P < 0.05$ and $P < 0.001$, respectively, compared to control HUVEC cells.

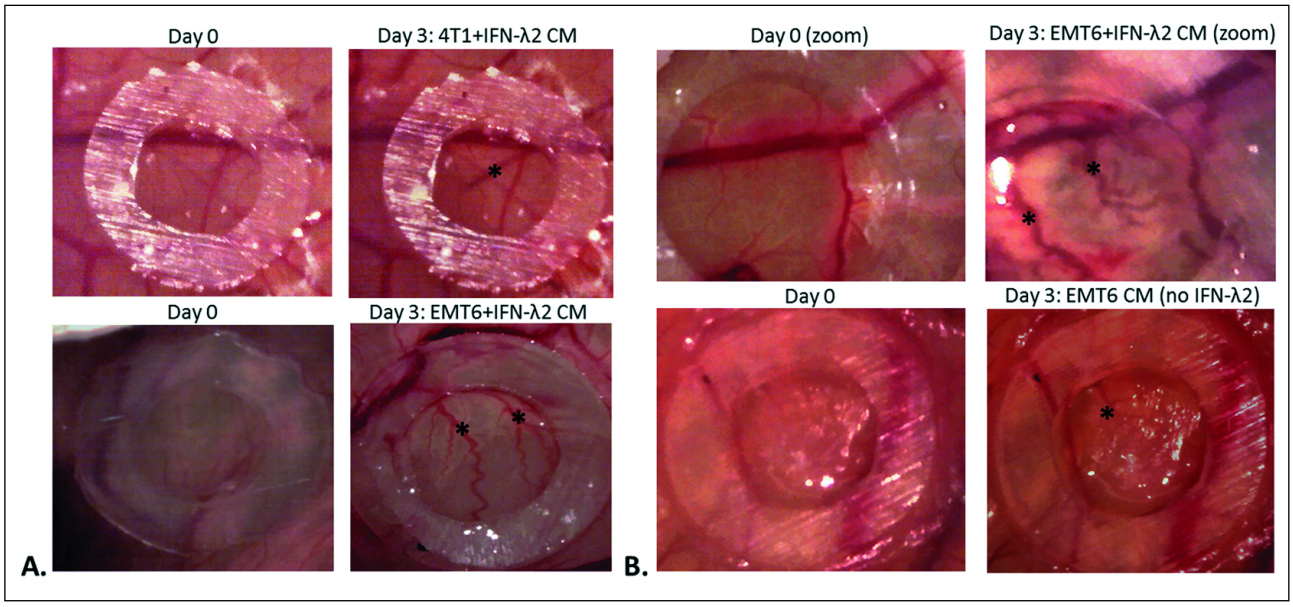

Fig. 4. CAM angiogenesis *in vivo* assay. (*A*) Blood vessels visible on CAM at day 0 (left panel) and 3 days after application into silicon ring 25 µl of conditioned medium (CM) of 4T1 either EMT6 cultured in IFN-λ2. The newly formed blood vessels are marked by asterisk. (*B*) Blood vessels visible on CAM at day 0 (left panel) and 3 days after application into silicon ring 25 µl conditioned medium by EMT6 cultured in IFN-λ2 (zoom) at the CAM (upper panel) and blood vessels visible on CAM 3 days after application into silicon ring 25 µl of EMT6 conditioned medium (CM) without IFN-λ2 pre-treatment. The newly formed blood vessels are marked by asterisk.

library was performed by means of molecular docking with FRED (OpenEye). After visual inspection of docking-based poses, 14 most promising compounds were selected, and submitted to *in vitro* evaluation.

The MTT assay showed relatively low cytotoxic activity of the most of these compounds on cancer cells (*Fig. 6*). Curcumin showed very strong cytotoxic activity on EMT6 cells decreasing their viability by 41% and 54% given at 10 and 20 µM concentration, respectively. When given at the concentration of 0.1 µM it reduced EMT6 cell viability by 10.2%. In case of 4T1 cells, it reduced their viability by 7.1%, 11.5% and 21.4%, at the following concentrations: 0.1 µM, 10 µM, 20 µM, respectively The 24-hydroxytormentic acid given at 2 µM, 6 µM and 8 µM concentration reduced viability of EMT6 cells by 0.9%, 5.3%, 11.4%, respectively. In 4T1 cells the same doses reduced viability by 2%, 6.9% and 8.1%, respectively. The viability of EMT6 cells treated with 6-prenyloaromadendrin at following concentrations: 2, 6, 8 µM was decreased by 17.2%, 18.5%,

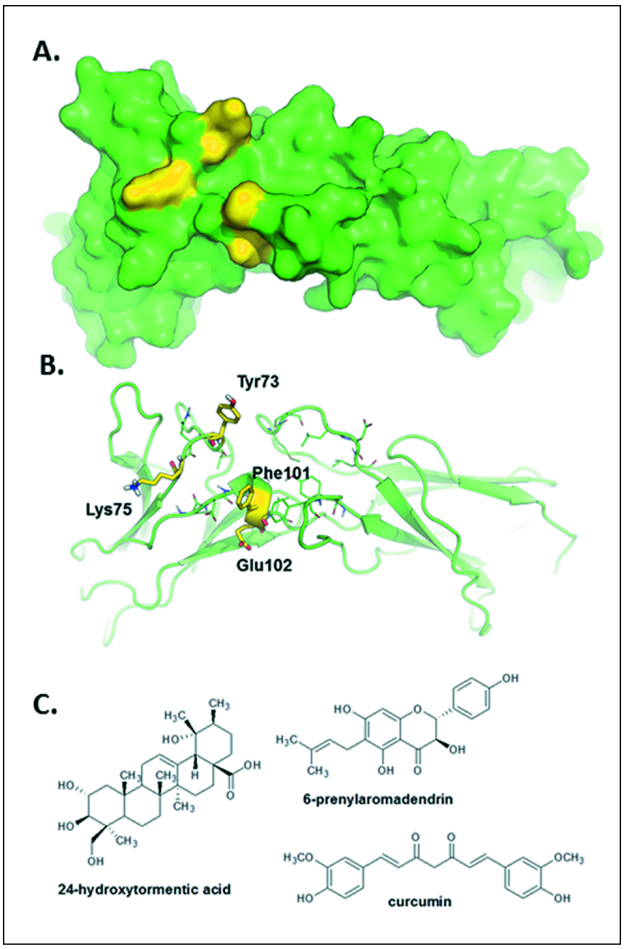

Fig. 5. Molecular modeling. (*A*, *B*) Binding site for small molecule inhibitors at IFN-λ2R identified in silico. The IFN-λ2R structure is showed as surface (*A*) and as cartoon, sticks and lines (*B*). Residues highlighted as possible hot-spots by the computational alanine scanning are colored yellow and labeled (*B*). (*C*) Chemical structure of active natural compounds identified by virtual screening and *in vitro* assays.

19%, respectively, compared with control cells; however in 4T1 cell line it was decreased by 3%, 4.5%, 1%, respectively, compared with control cells.

Selected inhibitors affect pro-angiogenic activity of interferon-λ2

In the *in vitro* angiogenesis assay we observed inhibition of tubule formation by medium conditioned with EMT6 and 4T1 cells treated with curcumin by 47% and 21.3%, respectively (compared with control cells treated with IFN-λ2) (*Fig. 7*). Treatment of EMT6 cells with 6-prenylaromadendrin and 24-hydroxytormentic acid caused 73.1% and 71.4% inhibition of tubule formation (compared with cells treated with IFN-λ2). In case of 4T1 treatment with 24-hydroxytormentic acid inhibited tubule formation by 50.4% and 6-prenylaromadendrin by 31% (compared with cells treated with IFN-λ2).

DISCUSSION

Despite the enormous advance in understanding of cancer biology, cancer is still one of the most common cause of death in Europe and United States. Based on the WHO reports, in 2012 cancer accounted for 8.2 million deaths worldwide. A slight improvement in treatment outcomes has prolonged patient life, however has not improved its quality. Patients with cancer often experience severe pain. It results not only from the tumor invasion in surrounding tissues, but also from the use of anticancer therapy with systemic effect (44). Therefore, it is important to still search for new strategies of more specific cancer treatment. These include compounds that inhibit tumor cell mobility (e.g. migrastatin analogues), off-DNA therapies against tumor-associated proteins (e.g. pyrazole derivates), and inhibitors of DNA lesions (e.g. DNA-dependent protein kinase inhibitors) (45-48). Because the blood vessels formation plays a crucial role in the tumor development, inhibitors of this process are interesting group of potential drugs. On the other hand, pro-angiogenic factors may be considered as prognostic markers. The VEGF expression in tumor tissue and in circulating endothelial progenitor cells in blood of tumor-bearing patients correlates with stage of cancer development (49, 50).

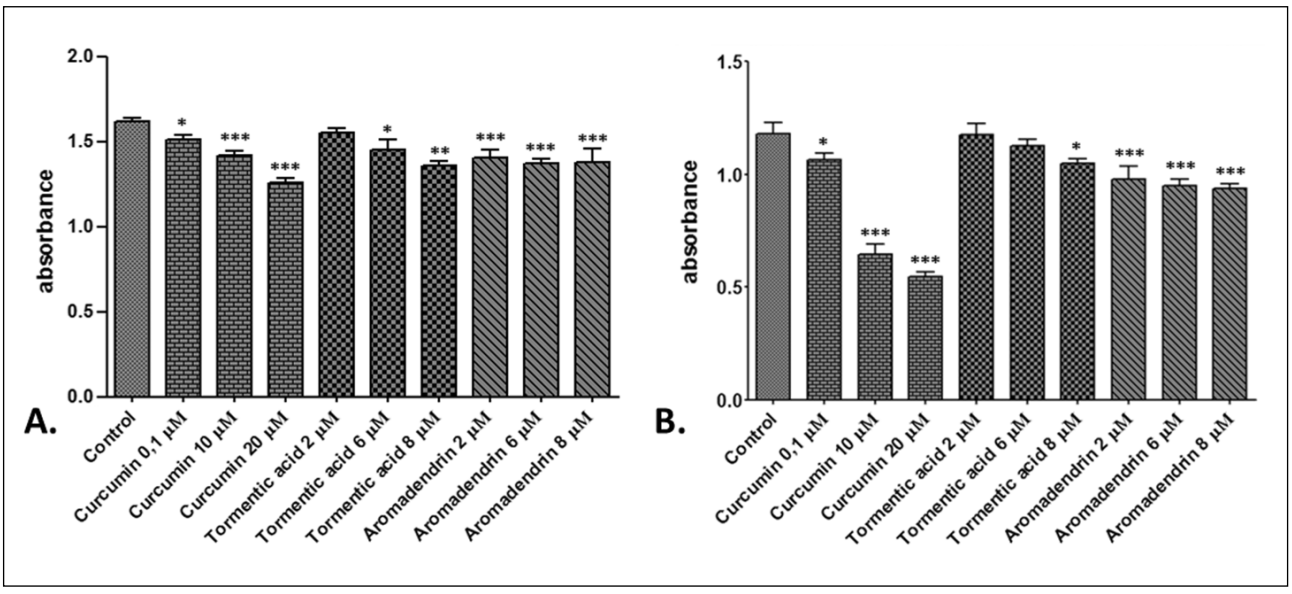

Fig. 6. MTT assay showing viability of 4T1 (*A*) and EMT6 (*B*) cells treated with inhibitors for 24 hours. The *P-value < 0.05 was regarded as significant whereas **P-value < 0.01 and ***P-value < 0.001 as highly significant relative to cancer cells.

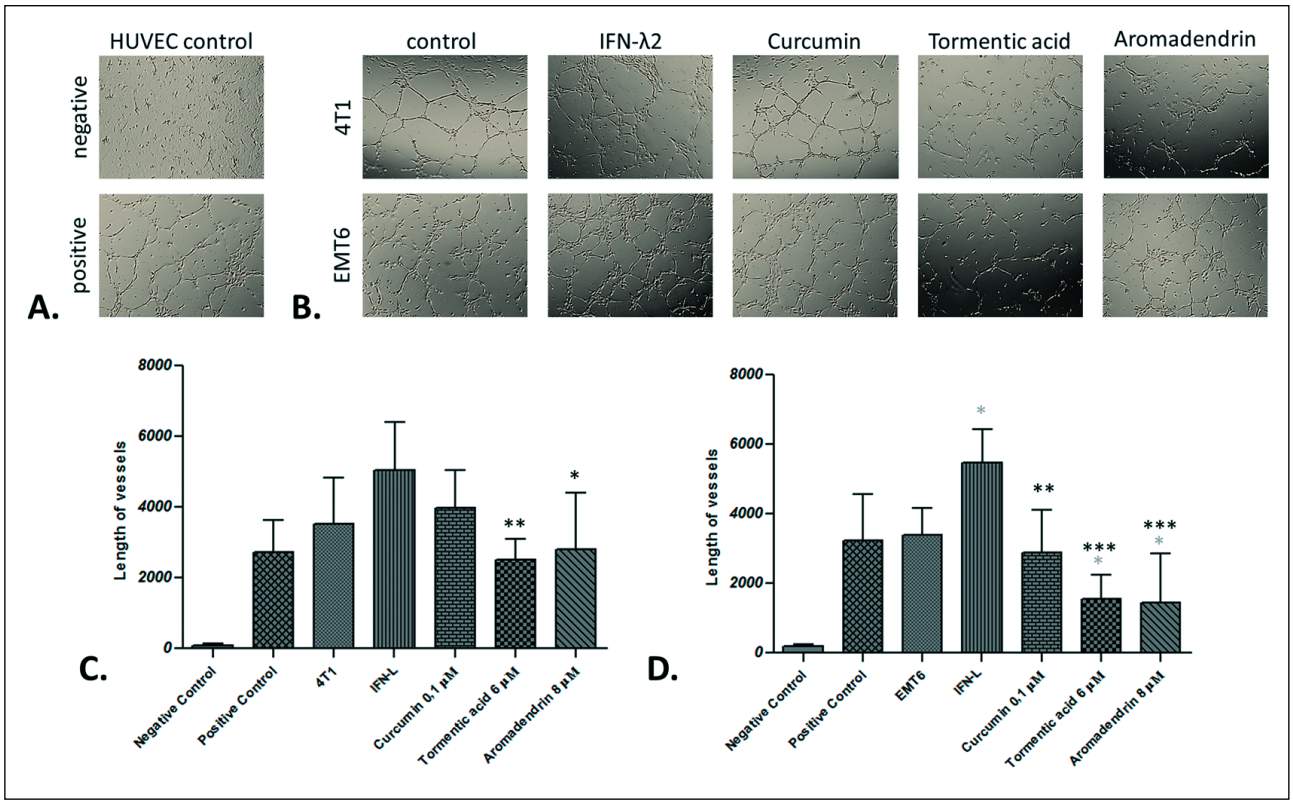

Fig. 7. (*A*) The pictures showing controls probes for angiogenic *in vitro* assay. (*B*) Representative microphotographs showing the tubule formation by HUVEC influenced mouse mammary cancer cells, mouse mammary cancer cells treated of IFN-λ2, mouse mammary cancer cells treated IFN-λ2 and inhibitors. (*C* and *D*) Graphs showing the length of formed vessel by HUVEC. The *P-value < 0.05 was regarded as significant whereas **P-value < 0.01 and ***P-value < 0.001 as highly significant relative to cancer cells. Grey * relative to 4T1/EMT6 group and black * relative to IFN-λ2 group.

However, tumor mass is not composed exclusively of the transformed cells, but also contains other untransformed, stromal and inflammatory cells. Among these are: fibroblasts, blood and lymphatic endothelial cells and immune cells. Tumor microenvironment cells contribute to the angiogenesis process by secretion of metalloproteinases, proangiogenic factors and proangiogenic switches (51). Particularly MDSCs have a high ability to promote angiogenesis (1-3). Our study demonstrated that MDSCs` (Gr-1$^+$CD11b$^+$CD45.2$^+$ cells) number in the lungs of mice with B16F10 tumors was significantly higher than in control mice (*Fig. 1A*). Similar trend has been observed in MDSCs' expression of *Ifn-λ2*. IFN-λ concentration in serum from tumor bearing mice has been studied. Until now it was shown that only in serum of patients with hepatocellular carcinoma the level of another IFN: IFN-γ is increased and correlates with the severity of the disease (52). We showed, that the level of IFN-λ2 in serum was significantly higher in mice with lymphoma (EL4) and melanoma (B76) compared with healthy animals (*Fig. 1C*). Despite level of IFN-λ2 in serum of mice with B16F10 melanoma was similar as in control mice, its expression was much higher in MDSCs (Gr-1$^+$CD11b$^+$CD45.2$^+$) isolated from the lungs of tumor-bearing mice as compared to controls (*Fig. 1*). Our previous study, conducted on tumor-bearing dogs, showed that expression of IFN-λ2 was significantly higher in MDSCs sorted from the blood of patients with advanced tumors than in these with cancer at the early stage (5). Therefore, we hypothesized that MDSCs may not necessarily secrete IFN-λ2 to the blood of tumor-bearing animals, but its secretion may be localized to particular tissues. Previously, we showed that co-culture of cancer cells with MDSCs increased expression of IFN-λ2R on canine mammary cancer cells. Supplementation of culture medium with IFN-λ2 also resulted in upregulation of IFN-λ2R expression to similar level (5). However, literature data suggests that IFN-λ2 may have both pro- and anti-tumor activity (5, 14-20, 22, 23), very likely depending on the tumor type and/or its stage of development. In order to clarify IFN-λ2 role in mammary cancer development, we investigated its influence on cancer cell migration and ability to new blood vessel formation. The migration test in Boyden chamber showed that IFN-λ2 significantly enhanced migration of EMT6 and 4T1 cancer cells. The use of IFN-λ2R blocking antibodies has reduced this effect. Similar results have been obtained by our team before on the canine mammary cancer cells and two human bladder cancer cell lines (5, 22). This effect may be related to increase of epithelial-mesenchymal transition in cancer cells due to stimulation with IFN-λ2. In our previous study we showed that IFN-λ2 increased expression of mesenchymal cells marker vimentin, and decreased expression of epithelial cells marker cytokeratin in cancer cells (5). However, another published data suggest that mammary epithelial cells with knockout of IFN-λ2R gene inoculated in mouse mammary fat pad decreased tumor growth (53).

In our previous study, we also demonstrated that IFN-λ2 was involved in tumor angiogenesis (5). In this study we evaluated a role of IFN-λ2 on the promotion of angiogenesis by mouse mammary cancer cells not only *in vitro*, but also *in ovo* on CAM. Results of the *in vitro* angiogenesis assay indicated that EMT6 and 4T1 cancer cells treated with IFN-λ2 significantly promoted

tubule formation by HUVECs. The length, size and number of new vessels was higher when HUVEC cells were cultured in medium conditioned with cancer cells pre-treated with IFN-λ2. Moreover, similar results were obtained in angiogenesis assay *in ovo*. Therefore, we conclude that IFN-λ2 influences cancer cells to stimulate angiogenesis. Previously we showed that increase of angiogenesis by IFN-λ2 was supposed to be a result of STAT-3 phosphorylation followed by higher expression of pro-angiogenic factors (5). The STAT3 is a strong regulator of expression of the pro-angiogenic factors such as: VEGF, matrix metalloproteinases (MMP-1, MMP-2, MMP-9) and bFGF (basic fibroblast growth factor) (54-57).

Because currently, there is no available molecular inhibitor of IFN-λ2 on the market, in order to identify possible natural inhibitors of the IFN-λ2/IFN-λ2R complex, we performed 3D molecular modeling and screening of the library of the natural products. After visual inspection of docking-based poses, 14 promising compounds were selected and submitted to the first round of *in vitro* evaluation. The first screening was performed based on their cytotoxic effect on cancer cells. Only three compounds did not promote cell proliferation: curcumin, 24-hydroxytormentic acid and 6-prenylaromadendrin (*Fig. 5C*). These molecules show relatively low cytotoxic activity on cancer cells. Only 6-prenylaromadendrin significantly affected metabolic activity of both cell lines at all concentrations (*Fig. 6*). High cytotoxic effect was observed also in case of curcumin at 10 and 20 μM concentrations. The results are consistent with the published data, because it is known that some of the flavonoids have antiproliferative properties. Antiproliferative effect of curcumin has been demonstrated on melanoma, breast and colon cancer cells. Curcumin inhibits translocation of NF-κB to the nucleus and decreases PDE1A, which is an UHRF1regulator. The consequence of this interaction is cell cycle arrest (58, 59). The 6-prenylaromadendrin, similarly to curcumin inhibits NF-κB activity and induces apoptosis by increase in expression of caspase 3 and 9 (60, 61). The 24-hydroxytormentic acid inhibits proliferation of melanoma, renal and prostate cancer cells (62, 63). It decreases NF-κB activity and increases caspase-dependent apoptosis (63, 64). For our further studies, the highest non-toxic concentrations of the examined compounds were used. To proof a role of IFN-λ2 in tumor angiogenesis, we treated endothelial cells with conditioned medium obtained from EMT6 and 4T1 cell lines pre-treated with the selected small molecular inhibitors of the IFN-λ2/IFN-λ2R complex. We showed significant inhibition of tubule formation by endothelial cells caused by all three compounds. Moreover, these compounds inhibited the effect caused by the IFN-λ2 supplementation in cancer cell culture medium. Similar effects were observed when instead of natural inhibitors we used specific blocking antibodies. Inhibition of tubule formation, that was observed in our study, may result not only from the block of the IFN-λ2 signaling *via* STAT-3 but also NF-κB. This pathway not only regulates the cell cycle, but also affects secretion of angiogenic factors: MMP-2, MMP-3, MMP-9 and it regulates expression of VEGF increasing proliferation and migration of endothelial cells. Inhibition of NF-κB may cause decline in adhesion molecules levels (ICAM-1 and ICAM-2) (65). Therefore, activity of the identified inhibitors is promising, however optimization and validation of new inhibitors is long process and needs further studies. If activity of these compounds will be successfully confirmed in further *in vivo* studies, the use of these inhibitors should be considered as anti-angiogenic therapy in cancer treatment. Our study showed that 4T1 cells were more resistant for the tested compounds than EMT6 cells. It is known that 4T1 cells are highly malignant (they represent mouse model of triple negative breast cancer) and very resistant to chemotherapy. Currently, their resistance to 6-thioguanine is used as a ‘gold standard’ in clonogenic metastasis assay (66).

To sum up, our study showed that IFN-λ2 enhances cancer cell migration and tumor angiogenesis. We showed, for the first time, that level of IFN-λ2 increased in serum of tumor-bearing mice. Moreover, we identified new promising small molecular inhibitors of IFN-λ2/IFN-λ2R interaction and confirmed their biological effect. Importantly, endothelial and bone marrow cells are unresponsive to IFN-λ2, what could make a therapy using its inhibitors more safe (15, 67).

Therefore IFN-λ2 may be an interesting target for further studies. Its mechanism of action requires clarification in various tumor types and stages of development.

Acknowledgements: The research described in this paper was funded by UMO-2013/09/D/NZ5/02496 grant from the National Science Centre. The publication was supported by the KNOW Consortium “Healthy Animals - Safe Food” (www.know.wmw.sggw.pl). The authors would like to acknowledge networking contribution by the COST Action CM1407 “Challenging organic syntheses inspired by nature - from natural products chemistry to drug discovery” (http://www.natchemdrugs.eu/index.php). The authors wish also to thank the OpenEye Free Academic Licensing Program for providing a free academic license for molecular modeling and chemoinformatics software.

Conflict of interest: None declared.

REFERENCES

1. Gabrilovich DI, Nagaraj S. Myeloid-derived suppressor cells as regulators of the immune system. *Nat Rev Immunol* 2009; 9: 162-174.
2. Schmid MC, Varner JA. Myeloid cells in the tumor microenvironment: modulation of tumor angiogenesis and tumor inflammation. *J Oncol* 2010; 2010: 201026. doi: 10.1155/2010/201026.
3. Youn J-I, Gabrilovich DI. The biology of myeloid-derived suppressor cells: The blessing and the curse of morphological and functional heterogeneity. *Eur J Immunol* 2010; 40: 2969-2975.
4. Kujawski M, Kortylewski M, Lee H, Herrmann A, Kay H, Yu H. Stat3 mediates myeloid cell dependent tumor angiogenesis in mice. *J Clin Invest* 2008; 118: 3367-3377.
5. Mucha J, Majchrzak K, Taciak B, Hellmen E, Krol M. MDSCs mediate angiogenesis and predispose canine mammary tumor cells for metastasis via IL-28/IL-28RA (IFN-λ) signaling. *PLoS One* 2014; 9: e103249. doi: 10.1371/journal.pone.0103249.
6. Uze G, Monneron D. IL-28 and IL-29: newcomers to the interferon family. *Biochimie* 2007; 89: 729-734.
7. Witte K, Witte E, Sabat R, Wolk K. IL-28A, IL-28B, and IL-29: promising cytokines with type I interferon-like properties. *Cytokine Growth Factor Rev* 2010; 21: 237-251.
8. O’Brien TR, Prokunina-Olsson L, Donnelly RP. IFN-λ4: the paradoxical new member of the interferon lambda family. *J Interferon Cytokine Res* 2014; 34: 829-838.
9. Brand S. IL-28A and IL-29 mediate antiproliferative and antiviral signals in intestinal epithelial cells and murine CMV infection increases colonic IL-28A expression. *Am J Physiol Gastrointest Liver Physiol* 2005; 289: G960-G968.
10. Ank N, Iversen MB, Bartholdy C, *et al*. An important role for type III interferon (IFN-lambda/IL-28) in TLR-induced antiviral activity. *J Immunol* 2008; 180: 2474-2485.
11. Thomas DL, Thio CL, Martin MP, *et al*. Genetic variation in IL28B and spontaneous clearance of hepatitis C virus. *Nature* 2009; 461(7265): 798-801.

12. Suppiah V, Moldovan M, Ahlenstiel G, *et al*. IL28B is associated with response to chronic hepatitis C interferon-λ and ribavirin therapy. *Nat Genet* 2009; 41: 1100-1104.
13. Steen HC, Gamero AM. Interferon-lambda as a potential therapeutic agent in cancer treatment. *J Interferon Cytokine Res* 2010; 30: 597-602.
14. Lasfar A, Abushahba W, Balan M, Cohen-Solal KA. Interferon lambda: a new sword in cancer immunotherapy. *Clin Dev Immunol* 2011; 2011: 349575. doi: 10.1155/2011/349575
15. Lasfar A, Gogas H, Zloza A, Kaufman HL, Kirkwood JM. IFN-λ cancer immunotheraphy: new kid on the block. *Immunotheraphy* 2016; 8: 877-888.
16. Lasfar A. Characterization of the mouse IFN-ligand-receptor system: IFN-s exhibit antitumor activity against B16 melanoma. *Cancer Res* 2006; 66: 4468-4477.
17. Zitzmann K, Brand S, Baehs S, *et al*. Novel interferon-lambdas induce antiproliferative effects in neuroendocrine tumor cells. *Biochem Biophys Res Commun* 2006; 344: 1334-1341.
18. Numasaki M, Tagawa M, Iwata F, *et al*. IL-28 elicits antitumor responses against murine fibrosarcoma. *J Immunol* 2007; 178: 5086-5098.
19. Fujie H, Tanaka T, Tagawa M, *et al*. Antitumor activity of type III interferon alone or in combination with type I interferon against human non-small cell lung cancer. *Cancer Sci* 2011; 102: 1977-1990.
20. Tezuka Y, Endo S, Matsui A, *et al*. Potential anti-tumor effect of IFN-λ2 (IL-28A) against human lung cancer cells. *Lung Cancer* 2012; 78: 185-192.
21. Lasfar A, Zloza A, de la Torre A, Cohen-Solal KA. IFN-λ: A new inducer of local immunity against cancer and infections. *Front Immunol* 2016; Dec 15 (7): 598. doi: 10.3389/fimmu.2016.00598.
22. Lee SJ, Lim JH, Choi YH, Kim WJ, Moon SK. Interleukin-28A triggers wound healing migration of bladder cancer cells via NF-κB-mediated MMP-9 expression inducing the MAPK pathway. *Cell Signal* 2012; 24: 1734-1742.
23. Lee SJ, Lee EJ, Kim SK, *et al*. Identification of pro-inflammatory cytokines associated with muscle invasive bladder cancer; the roles of IL-5, IL-20, and IL-28A. *PLoS One* 2012; 7: e40267. doi: 10.1371/journal.pone.0040267
24. Novak AJ, Grote DM, Ziesmer SC, Rajkumar V, Doyle SE, Ansell SM. A role for IFN-λ1 in multiple myeloma B cell growth. *Leukemia* 2008; 22: 2240-2246.
25. Miknis ZJ, Magracheva E, Li W, Zdanov A, Kotenko SV, Wlodawer A. Crystal structure of human interferon-λ1 in complex with its high-affinity receptor interferon- λR1. *J Mol Biol* 2010; 404: 650-664.
26. Sali A, Blundell TL. Comparative protein modelling by satisfaction of spatial restraints. *J Mol Biol* 1993; 234: 779-815.
27. Case DA, Darden TA, Cheatham TE, *et al*. AMBER 12. Reference Manual. San Francisco, University of California 2012.
28. Cau Y, Fiorillo A, Mori M, Ilari A, Botta M, Lalle M. Molecular dynamics simulations and structural analysis of Giardia duodenalis 14-3-3 protein-protein interactions. *J Chem Inf Model* 2015; 55: 2611-2622.
29. Sholokh M, Improta R, Mori M, *et al*. Tautomers of a fluorescent G surrogate and their distinct photophysics provide additional information channels. *Angew Chem Int Ed Engl* 2016; 128: 8106-8110.
30. Cau Y, Mori M, Supuran CT, Botta M. Mycobacterial carbonic anhydrase inhibition with phenolic acids and esters: kinetic and computational investigations. *Org Biomol Chem* 2016; 14: 8322-8330.
31. Miller BR, McGee TD, Swails JM, Homeyer N, Gohlke H, Roitberg AE. MMPBSA.py: an efficient program for end-state free energy calculations. *J Chem Theory Comput* 2012; 8: 3314-3321.
32. McGann M. FRED pose prediction and virtual screening accuracy. *J Chem Inf Model* 2011; 51: 578-596.
33. FRED 3.0.1 OpenEye Scientific Software, Santa Fe, NM, U.S.A. Available from: http://www.eyesopen.com.
34. Hawkins PC, Skillman AG, Warren GL, Ellingson BA, Stahl MT. Conformer generation with OMEGA: algorithm and validation using high quality structures from the Protein Databank and Cambridge Structural Database. *J Chem Inf Model* 2010; 50: 572-584.
35. OMEGA Release 2.5.1.4: OpenEye Scientific Software, Santa Fe, NM, U.S.A. Available from: http://www.eyesopen.com).
36. Ohtani K, Kasai R, Yang CR, Yamasaki K, Zhou J, Tanaka O. Oleanane glycosides from roots of Glycyrrhiza yunnanensis. *Phytochemistry* 1994; 36: 139-145.
37. Ingham JL, Tahara S, Dziedzic SZ. New 3-hydroxyflavanone (dihydroflavonol) phytoalexins from the papilionate legume Shuteria vestita. *J Nat Prod* 1986; 49: 631-638.
38. Hess SC, Monache FD. Divergioic acid, a triterpene from Vochysia divergens. *J Braz Chem Soc* 1999; 10: 104-106.
39. Ango PY, Kapche DW, Fotso GW, *et al*. Thonningiiflavanonol A and thonningiiflavanonol B, two novel flavonoids, and other constituents of Ficus thonningii Blume (Moraceae). *Z Naturforsch C* 2016; 71: 65-71.
40. Infante P, Mori M, Alfonsi R, *et al*. Gli1/DNA interaction is a druggable target for Hedgehog-dependent tumors. *EMBO J* 2015; 34: 200-217.
41. Cirigliano A, Stirpe A, Menta S, *et al*. Yeast as a tool to select inhibitors of the cullin deneddylating enzyme Csn5. *J Enzyme Inhib Med Chem* 2016; 31: 1632-1637.
42. Infante P, Alfonsi R, Ingallina C, *et al*. Inhibition of Hedgehog-dependent tumors and cancer stem cells by a newly identified naturally occurring chemotype. *Cell Death Dis* 2016; 7: e2376. doi: 10.1038/cddis.2016.195
43. Mascarello A, Mori M, Chiaradia-Delatorre LD, *et al*. Discovery of Mycobacterium tuberculosis protein tyrosine phosphatase B (PtpB) inhibitors from natural products. *PLoS One* 2013; 8: e77081. doi: 10.1371/journal.pone.0077081
44. Leppert W, Zajaczkowska R, Wordliczek J, Dobrogowski J, Woron J, Krzakowski M. Pathophysiology and clinical characteristics of pain in most common locations in cancer patients. *J Physiol Pharmacol* 2016; 67: 787-799.
45. Majchrzak K, Lo Re D, Gajewska M, *et al*. Migrastatin analogues inhibit canine mammary cancer cell migration and invasion. *PLoS One* 2013; 8: e76789. doi: 10.1371/journal.pone.0076789
46. Lo Re D, Zhou Y, Mucha J, *et al*. Synthesis of migrastatin analogues as inhibitors of tumour cell migration: exploring structural change in and on the macrocyclic ring. *Chemistry* 2015; 21: 18109-18121.
47. Lehmann TP, Kujawski J, Kruk J, Czaja K, Bernard MK, Jagodzinski PP. Cell-specific cytotoxic effect of pyrazole derivatives on breast cancer cell lines MCF7 and MDA-MB-231. *J Physiol Pharmacol* 2017; 68: 201-207.
48. Pospisilova M, Seifrtova M, Rezacova M. Small molecule inhibitors of DNA-PK for tumor sensitization to anticancer therapy. *J Physiol Pharmacol* 2017; 68: 337-344.
49. Nishida N, Yano H, Nishida T, Kamura T, Kojiro M. Angiogenesis in cancer. *Vasc Health Risk Manag* 2006; 2: 213-219.
50. Rhone P, Ruszkowska-Ciastek B, Celmer M, *et al*. Increased number of endothelial progenitors in peripheral blood as a possible early marker of tumour growth in post-menopausal breast cancer patients. *J Physiol Pharmacol* 2017; 68: 139-148.
51. Quail DF, Joyce JA. Microenvironmental regulation of tumor progression and metastasis. *Nat Med* 2013; 19: 1423-1437.

52. Lee IC, Huang YH, Chau GY, *et al*. Serum interferon gamma level predicts recurrence in hepatocellular carcinoma patients after curative treatments: interferon-gamma and HCC. *Int J Cancer* 2013; 133: 2895-2902.
53. Burkart C, Arimoto K, Tang T, *et al*. Usp18 deficient mammary epithelial cells create an antitumour environment driven by hypersensitivity to IFN-λ and elevated secretion of Cxcl10: Usp18 deficiency alters tumour environment. *EMBO Mol Med* 2013; 5: 1035-1050.
54. Xie T, Wei D, Liu M, *et al*. Stat3 activation regulates the expression of matrix metalloproteinase-2 and tumor invasion and metastasis. *Oncogene* 2004; 23: 3550-3560.
55. Itoh M, Murata T, Suzuki T, *et al*. Requirement of STAT3 activation for maximal collagenase-1 (MMP-1) induction by epidermal growth factor and malignant characteristics in T24 bladder cancer cells. *Oncogene* 2006; 25: 1195-1204.
56. Chen Z, Han ZC. STAT3: a critical transcription activator in angiogenesis. *Med Res Rev* 2008; 28: 185-200.
57. Song Y, Qian L, Song S, *et al*. Fra-1 and Stat3 synergistically regulate activation of human MMP-9 gene. *Mol Immunol* 2008; 45: 137-143.
58. Mehta K, Pantazis P, McQueen T, Aggarwal BB. Antiproliferative effect of curcumin (diferuloylmethane) against human breast tumor cell lines. *Anticancer Drugs* 1997; 8: 470-481.
59. Wuerzberger-Davis SM, Chang PY, Berchtold C, Miyamoto S. Enhanced G2-M arrest by nuclear factor-(kappa)B-dependent p21waf1/cip1 induction. *Mol Cancer Res* 2005; 3: 345-353.
60. Zhang WY, Lee JJ, Kim IS, Kim Y, Myung CS. Stimulation of glucose uptake and improvement of insulin resistance by aromadendrin. *Pharmacology* 2011; 88: 266-274.
61. Duh PD, Chen ZT, Lee SW, *et al*. Antiproliferative activity and apoptosis induction of Eucalyptus Citriodora resin and its major bioactive compound in melanoma B16F10 cells. *J Agric Food Chem* 2012; 60: 7866-7872.
62. Fogo AS, Antonioli E, Calixto JB, Campos AH. Tormentic acid reduces vascular smooth muscle cell proliferation and survival. *Eur J Pharmacol* 2009; 615: 50- 54.
63. Loizzo MR, Bonesi M, Passalacqua NG, Saab A, Menichini F, Tundis R. Antiproliferative activities on renal, prostate and melanoma cancer cell lines of Sarcopoterium spinosum aerial parts and its major constituent tormentic acid. *Anticancer Agents Med Chem* 2013; 13: 768-776.
64. Zhang TT, Yang L, Jiang JG. Tormentic acid in foods exerts anti-proliferation efficacy through inducing apoptosis and cell cycle arrest. *J Funct Foods* 2015; 19: 575-583.
65. Tabruyn SP, Griffioen AW. NF-κB: a new player in angiostatic therapy. *Angiogenesis* 2008; 11: 101-106.
66. Pulaski BA, Ostrand-Rosenberg S. Mouse 4T1 breast tumor model. In: Current Protocols in Immunology. JE Coligan, BE Bierer, DH Margulies, *et al*. (eds). Hoboken, NJ, U.S.A., John Wiley & Sons Inc. 2001.
67. Witte K, Gruetz G, Volk H-D, *et al*. Despite IFN-λ receptor expression, blood immune cells, but not keratinocytes or melanocytes, have an impaired response to type III interferons: implications for therapeutic applications of these cytokines. *Genes Immun* 2009; 10: 702-714.

Received: June 14, 2017
Accepted: August 25, 2017

Author's address: Prof. Magdalena Krol, Warsaw University of Life Sciences, Department of Physiological Sciences, Faculty of Veterinary Medicine, 159 Nowoursynowska Street, 02-787, Warsaw, Poland.
E-mail: magdalena_krol@sggw.pl